Vector boson production in ATLAS

Lashkar Kashif on behalf of the ATLAS Collaboration
Department of Physics
University of Wisconsin, Madison
Wisconsin, USA

1 Introduction

The production of massive vector bosons (W and Z) is one of the most important processes in ATLAS. There are both theoretical and experimental motivations for studying the properties of these bosons.

From an experimental viewpoint, W and Z decays are vital for benchmarking the detector, allowing us to assess the response of the detector hardware and software. We can use their decay products to measure efficiencies of lepton triggers and reconstruction, energy and angular resolution, energy scales etc.

From a theoretical perspective, predictions accurate to next-to-leading-order (NLO) or next-to-next-to-leading-order (NNLO) in QCD are available for many of the measurements involving W and Z bosons. These predictions can be tested in both high- and low-Q^2 regimes by comparing with measured quantities. In addition, measurement of the W charge asymmetry and Z rapidity spectrum can help constrain the parton distribution functions (PDFs) of the proton. Indeed, some of the measurements made by ATLAS are already sensitive to differences among different PDF sets.

Particles in many Beyond the Standard Model physics scenarios decay into high transverse momentum (p_{T}) W and Z bosons. Hint of new physics can therefore show up in the tails of W or Z p_{T} spectra.

In these proceedings, we present the results of three sets of measurements involving the vector bosons:

- W and Z total cross sections
- W decay lepton charge asymmetry
- Z differential cross section in p_{T} bins

The data samples used in these analyses were collected by ATLAS during 2010, and correspond to about 35 pb^{-1} of integrated luminosity depending on the analysis. The error on the luminosity measurement is 3.4% [1].

2 Common event selection

In all analyses the following selection criteria are applied:

- Trigger: Single electron trigger with a threshold of E_{T}=15 GeV for electron channels; single muon trigger with a threshold of p_{T}=13 GeV for muon channels.
- Cosmic muon rejection: Events are required to have at least one primary vertex with three or more associated tracks. The longitudinal impact parameter of any lepton in the event must be within 1 cm of the z position of the vertex.
- Muon selection: The muon is required to be a *combined* muon, reconstructed using information from both the inner detector (ID) and the muon spectrometer (MS). It must have $p_{\mathrm{T}} > 20$ GeV and be within the pseudorapidity region $|\eta| < 2.4$. Finally, cuts are applied to the ID-MS track matching quality, impact parameter and isolation.
- Electron selection: Electron reconstruction uses information from calorimeter clusters and associated ID tracks. Each electron is required to have $p_{\mathrm{T}} > 20$ GeV and $|\eta| < 2.47$. In the case of the $Z \to ee$ cross section, the η selection criterion of one of the two electrons is extended to the region $2.5 < |\eta| < 4.9$. There is a cut on the electron isolation in the calorimeter.

Additional selection criteria are applied to reduce background and define signal regions:

- $W \to l\nu$ analyses: missing transverse energy, $E_{\mathrm{T}}^{\mathrm{miss}} > 25$ GeV, and transverse mass $m_{\mathrm{T}} > 40$ GeV, where $m_{\mathrm{T}} = \sqrt{2p_{\mathrm{T}}^{\mathrm{l}} E_{\mathrm{T}}^{\mathrm{miss}}(1-\cos(\phi^{\mathrm{l}} - \phi^{\nu}))}$.
- $Z \to ll$ analyses: dilepton invariant mass $66 < m_{ll} < 116$ GeV.

3 Backgrounds

In all analyses, QCD multijet background is determined from data, but the methods used vary among the analyses (see Section IV of [3]). In the $W \to e\nu$ channel, a template fit to the $E_{\mathrm{T}}^{\mathrm{miss}}$ distribution is used. The $W \to \mu\nu$ channel employs QCD control regions defined in a 2-dimensional phase space of muon isolation and $E_{\mathrm{T}}^{\mathrm{miss}}$. The $Z \to ee$ channel uses a set of loosened electron selection criteria to obtain a QCD-rich event sample. A fit to the ee invariant mass distribution in this sample yields the QCD contamination in the signal region. Finally, the $Z \to \mu\mu$ channel uses QCD control regions defined by muon isolation and $m_{\mu\mu}$.

4 Lepton performance evaluation

$Z \to ll$ events are used to estimate electron and muon trigger and reconstruction efficiencies as well as the resolution and scale of electron E_{T} and muon p_{T}. Trigger and reconstruction efficiencies are obtained using the tag-probe approach [2]. Fits to dilepton invariant mass distributions are used to extract electron E_{T} and muon p_{T} resolution and scale. These quantities in general differ between data and simulation; event- and lepton-level corrections are applied to the simulation in all analyses to take these differences into account.

5 Results

5.1 W, Z total cross sections

Figure 1 [3] shows the measured W^+, W^-, $W^\pm$ and Z fiducial cross sections with error ellipses, compared with theoretical predictions using several different PDF sets. In all cases, we see good agreement between observation and prediction.

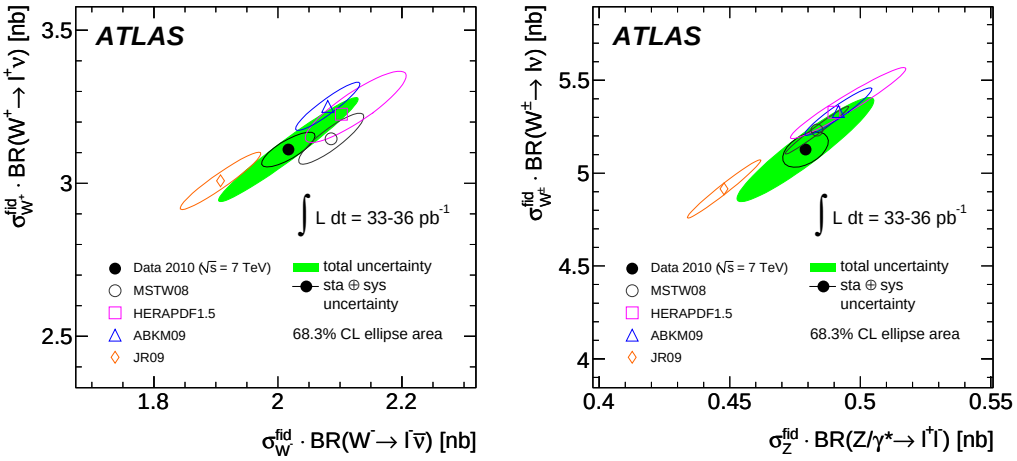

Figure 1: *Left*: W^+ fiducial cross section vs W^- fiducial cross section; *right*: $W^\pm$ fiducial cross section vs Z fiducial cross section. In both cases, the measured cross section is compared with theoretical prediction using four different PDF sets. The uncertainties on the theoretical predictions correspond to PDF uncertainties only.

5.2 Charge asymmetry of leptons from W decay

Figure 2 [3] shows the lepton charge asymmetry in W decays as a function of lepton pseudorapidity. Theoretical predictions using four different PDF sets are also shown.

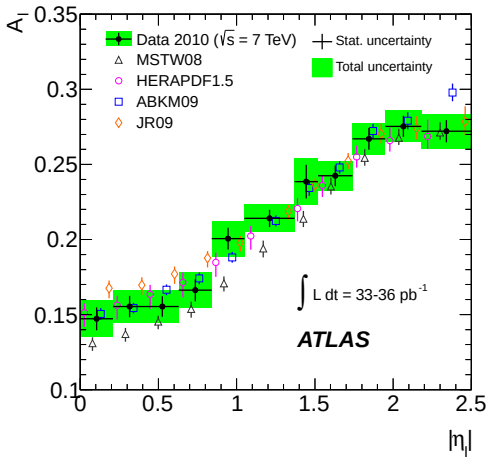

Figure 2: Charge asymmetry of leptons in W decays as a function of the lepton η compared with theoretical prediction accurate to *NNLO*.

5.3 Z differential cross section $d\sigma/dp_{\mathrm{T}}$

Figure 3 [4] shows the results of the $d\sigma/dp_{\mathrm{T}}^{\mathrm{Z}}$ measurement. Within statistical uncertainty, the observed spectrum shows fairly good agreement with the predictions.

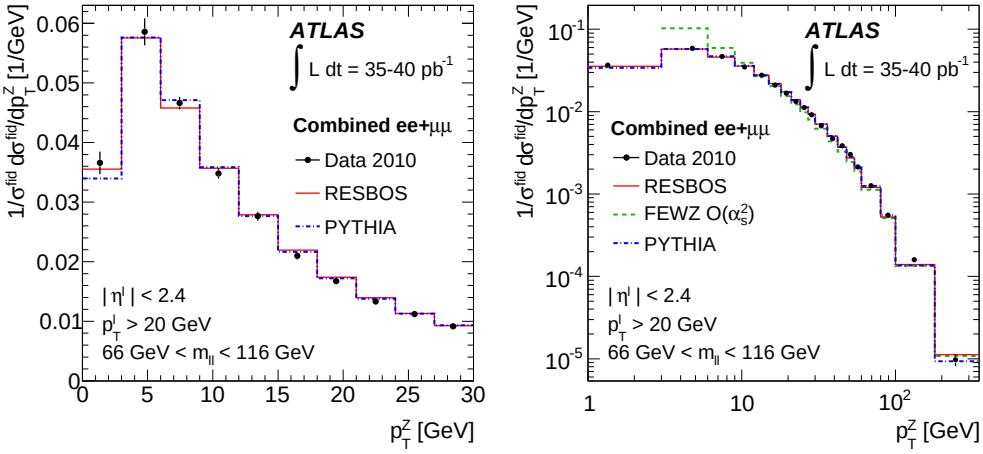

Figure 3: Z boson p_{T} spectrum in the range $0 < p_{\mathrm{T}}^{\mathrm{Z}} < 30$ GeV *(left)* and in the range $0 < p_{\mathrm{T}}^{\mathrm{Z}} < 300$ GeV *(right)*.

References

[1] ATLAS Collaboration, ATLAS Note, **ATLAS-CONF-2011-011**, (2011), http://cdsweb.cern.ch/record/1334563.

[2] ATLAS Collaboration, ATLAS Note, **ATLAS-CONF-2011-063**, (2011), http://cdsweb.cern.ch/record/1345743.

[3] ATLAS Collaboration, (2011), submitted to PRD, arXiv:1109.5141 [hep-ex].

[4] ATLAS Collaboration, (2011), accepted by PLB, arXiv:1107.2381 [hep-ex].